Received: 20 May 2023 | Revised: 12 January 2024 | Accepted: 16 January 2024

DOI: 10.1002/dep2.273

The Depositional Record
A journal of the International Association of Sedimentologists
Open Access
IAS
WILEY

ORIGINAL RESEARCH ARTICLE

Gypsum lakes, sandflats and soils revealed from the Triassic Red Peak Formation of the Chugwater Group, north-central Wyoming

Maya Yamei Bradford | **Kathleen C. Benison**

Department of Geology and Geography, West Virginia University, Morgantown, West Virginia, USA

Correspondence
Maya Yamei Bradford, Department of Geology and Geography, West Virginia University, 98 Beechurst Ave., Morgantown, WV 26505, USA.
Email: myb00001@mix.wvu.edu

Funding information
SEPM Rocky Mountain Section Edwin D. McKee Grant and a West Virginia University Geology Student Field Experience Fund grant to MYB

Abstract

Bedded gypsum is relatively common in bedded evaporites associated with red bed siliciclastics of Permo-Triassic Pangea. However, little attention has been paid to the textures of ancient gypsum, which can be used to refine interpretations of depositional environment and diagenetic history. This project describes the textures of bedded gypsum from an outcrop of the Triassic Red Peak Formation (Chugwater Group) near Greybull, Wyoming. Fieldwork, petrography and X-ray diffraction reveal three distinct lithologies of bedded gypsum: bottom-growth gypsum, laminated gypsum and clastic gypsum. Bottom-growth gypsum precipitated at the bottom of shallow saline surface water bodies. Laminated gypsum probably formed in shallow saline lakes and mudflats. Clastic gypsum units are composed of aeolian-reworked bottom-growth gypsum crystals deposited in sandflats. Red siliciclastic mudstones are characterised by their massive nature and abundant blocky peds. Detailed study of this outcrop of the Red Peak Formation shows that it formed in shallow saline lakes and associated mudflats, sandflats and desert soils.

KEYWORDS

aeolian, Chugwater, continental, gypsum, lakes, palaeosols, Pangea, Red Peak

1 | INTRODUCTION

Bedded evaporites and associated red bed siliciclastics from the mid Permian through early Triassic periods are widespread across equatorial Pangea. These rocks are representative of extensive continental acid-saline lake and groundwater systems in arid, desert landscapes (Benison et al., 1998; Benison & Goldstein, 2002; Andeskie et al., 2018). These end-member environments of acid brines in dry climates appear to have been long-lived, geographically widespread systems, probably representing a major component of Pangea. Knowledge of continental environmental, biological and climate conditions during the Permo-Triassic is relevant for three general reasons: (1) these may be among the most geochemically extreme environments known on Earth; (2) the end-Permian time experienced the greatest loss of species; and (3) the late Palaeozoic was the last time there was a major icehouse to greenhouse transition (Stanley & Yang, 1994; Parrish, 1995; Gastaldo et al., 1996;

Benison et al., 1998; Payne & Clapham, 2012; Montañez & Poulsen, 2013; Benison & Bowen, 2015; Dietl et al., 2015; Vajda et al., 2020).

In northern Wyoming, the Goose Egg Formation and Chugwater Group make up most of the mid Permian—early Triassic depositional record. The Red Peak Formation is the lowest formation of the Chugwater Group, considered to be approximately 170 m thick, and composed of red beds and bedded gypsum (Maughn, 1972; Figure 1). While the Chugwater Group and its distinctive bright-red colour are well-known to geologists familiar with Wyoming, the interpreted depositional environments remain contentious (Branson, 1915; Cavaroc & Flores, 1917; High & Picard, 1969; Picard, 1967; Irmen & Vondra, 2000; Lovelace & Lovelace, 2012; Knapp et al., 2015, 2016; Knapp, 2020). The bedded gypsum of the Chugwater Group has not yet been described in sedimentological detail; ancient bedded gypsum, in general, is understudied.

The objective of this study was to characterise the sedimentology and make detailed depositional interpretations of bedded gypsum from an outcrop of the Red Peak Formation in north-central Wyoming. Fieldwork, mineral identification and thin-section petrography were used.

2 | BACKGROUND

2.1 | Textures of gypsum

Bedded gypsum is a term used for depositional gypsum. It includes (1) bottom-growth gypsum, beds of vertically oriented bladed or acicular crystals that form at the bottom of $CaSO_4$-rich surface waters such as lakes, lagoons or marine basins; (2) cumulate gypsum, crystals that precipitate at the air–water interface, in the water column or at the boundary between layers of salinity-stratified water, and settle at the bottom of the water body; and (3) clastic gypsum, grains of reworked gypsum crystals (Hardie & Eugster, 1971; Schreiber & Kinsman, 1975; Schreiber et al., 1976; Schreiber, 1987; Schreiber & El Tabakh, 2000; Benison et al., 2007).

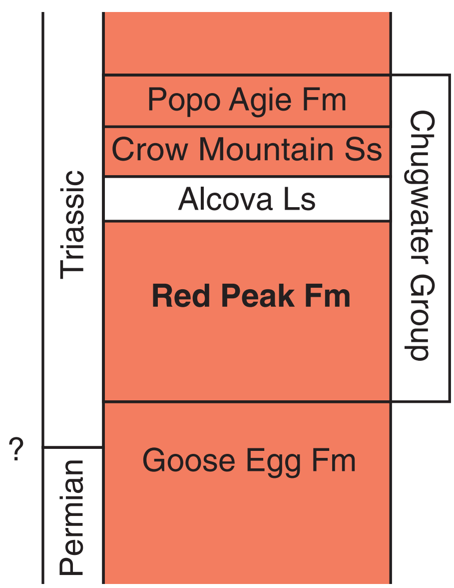

FIGURE 1 Stratigraphic nomenclature of the Chugwater Group and its four formations, modified after Knapp (2020).

Gypsum can also form diagenetically. Displacive gypsum is acicular or lath-shaped gypsum crystals, randomly oriented in a siliciclastic or carbonate sediment. They precipitate from shallow $CaSO_4$-rich groundwaters in uncemented sediment (Smoot & Lowenstein, 1991; Andeskie & Benison, 2020). $CaSO_4$-rich groundwaters can also precipitate gypsum intergranular cement and gypsum vein-filling cement. Additionally, gypsum can also undergo neomorphism. For example, gypsum bottom-growth crystals from the Triassic Mercia Mudstone Group of Northern Ireland have been replaced by halite (Andeskie et al., 2018). Gypsum and anhydrite undergo hydration and dehydration changes, as seen in the Permian Blaine Formation of Kansas (Benison, 1997).

The textures of gypsum have been well-documented from modern environments, as well as Miocene deposits (Schreiber & Kinsman, 1975; Schreiber, 1987; Benison et al., 2007; Kiro et al., 2016; Knapp et al., 2016; Langford et al., 2016; Benison, 2019a). Modern examples include bottom-growth, cumulate, clastic and displacive gypsum from acid-saline lake systems in Western Australia, bottom-growth and clastic gypsum from acid-saline lake systems in northern Chile, and clastic gypsum from sandflats and dunes at White Sands National Monument in New Mexico, USA (McKee, 1966; Benison et al. 2007; Langford et al., 2016; Benison, 2019a). Miocene examples include bottom-growth gypsum from Egypt and bottom-growth gypsum and laminated gypsum from Italy (Attia et al., 1995; Manzi et al., 2009; Lugli et al., 2010; Dela Pierre et al., 2011). However, there remains a paucity of published studies of the textures of bedded gypsum from Mesozoic, Palaeozoic and Precambrian rocks.

2.2 | The Chugwater Group

The Red Peak Formation is the lowest of four formations of the Chugwater Group (Figure 1). Rocks of the Chugwater Group are well-exposed around the flanks of Laramide uplifts in north-central Wyoming. Descriptions of the Chugwater note its distinctive red colour, fine grain size, reptile trackways, the presence of gypsum, and its assumed lateral continuity and consistent thickness

(Branson, 1915; Tomlinson, 1916; Picard, 1967; High & Picard, 1969; Irmen & Vondra, 2000; Lovelace & Lovelace, 2012).

Sedimentological observations of the Chugwater Group have focussed on the siliciclastics. Field and petrographic studies by Knapp (2020) interpreted the red bed siliciclastics of the Red Peak Formation as episodic sheet flood deposits on alluvial plains that underwent pedogenesis. The abundance of palaeosols strongly suggests a continental origin for this sequence of Permo-Triassic red beds and bedded gypsums. Yet, the textures of the bedded gypsums of these rocks remained undescribed.

The upper portion of the Red Peak Formation near Greybull, Wyoming, is characterised by alternating units of bedded gypsum and red bed siliciclastic mudstone. Are depositional textures preserved in this ancient bedded gypsum? Is all bedded gypsum the same? Can we interpret depositional environments from the bedded gypsum units? Or, has all or some gypsum succumbed to diagenetic alteration that obliterates depositional textures? The main objective of this study was to make detailed petrographic descriptions of the bedded gypsum units at one outcrop of the Red Peak Formation, and from those descriptions, interpret depositional environments.

3 | METHODS

Fieldwork, petrography and mineral identification were used to characterise the bedded gypsum at one outcrop of the Red Peak Formation near Greybull, Wyoming (Figure 2). Observations were used to form interpretations of depositional environments and diagenetic features.

Multiple exposures of the Red Peak Formation near Greybull in north-central Wyoming were visited in June of 2021. The Red Peak Formation is exposed as outcrops and quarry walls. Each exposure observed in this area was composed of alternating units of red bed siliciclastics and bedded gypsum. After preliminary investigation of several outcrops near Greybull, including quarry exposures at a Georgia-Pacific Gypsum mine, one *ca* 9 m thick outcrop was chosen for a detailed study of textural observations.

The study outcrop is approximately 8 km north of Greybull, Wyoming (Figure 2). It is the closest to Greybull County Road #26. The outcrop is near, but stratigraphically above, a Wyo-Ben, Inc. stucco plant, which processes bentonite. The GPS co-ordinates for this outcrop are 44°34′52.06″ north, 108°7′38.22″ west. This outcrop is approximately 50 m below a pale-grey carbonate unit interpreted as the Alcova Limestone. The study outcrop is exposed on the western limb of the Sheep Mountain Anticline (Forster et al., 1996; Figure 2).

A centimetre-scale measured section was performed at the outcrop. Field notes and digital photographs were used to document observations. Colour was determined using a Munsell Soil Chart. Hydrochloric acid, field X-ray fluorescence (XRF), X-ray diffraction (XRD) and petrography were used to test for elemental and mineral composition. Representative hand samples were collected and returned to West Virginia University. Field and petrographic observations included descriptions of sedimentary textures, sedimentary structures, mineral composition, colour, optical properties, any fossils, stratigraphic contacts and diagenetic features.

Samples collected in the field were slabbed on a rock saw and made into 16 large-format thin sections. Thin sections were prepared at Spectrum Petrographics, Inc., and were made with minimal use of water or heat. Some samples were vacuum impregnated with blue epoxy. Thin sections were observed and photographed under transmitted, reflected and polarised light with an Olympus BX53 microscope, using 6.3–63× magnification.

Rock samples were powdered and analysed using XRD to identify minerals. Three samples of representative bedded gypsum units were analysed by XRD using bulk analysis by K/T Geoservices, Inc. In the field, some bedded gypsum was tested for elemental composition with a Bruker handheld XRF. Additional mineralogy data were reported from Georgia-Pacific Gypsum mine geologists.

4 | RESULTS AND INTERPRETATIONS

The study outcrop is composed of alternating units of bedded gypsum and red siliciclastic mudstone (Figure 3). Here, beds are defined as individual depositional layers, and units are considered assemblages of similar beds. Of the eight units of bedded gypsum here, field and petrographic observations reveal three lithologies of bedded gypsum. Additionally, all red bed units were similar to one another (Figure 3). The three bedded gypsum lithologies are bottom-growth gypsum, laminated gypsum and clastic gypsum.

4.1 | Lithologies and interpreted depositional environments

4.1.1 | Bottom-growth gypsum lithology: Saline lake lithofacies

Results

This bedded gypsum lithology is pale orange (5 YR 8/4) in outcrop and grey (GLEY 2 7/1 10B) to yellowish white (7.5 YR 8/1) with streaks of pale red (10 R 7/4) and yellow (2.5

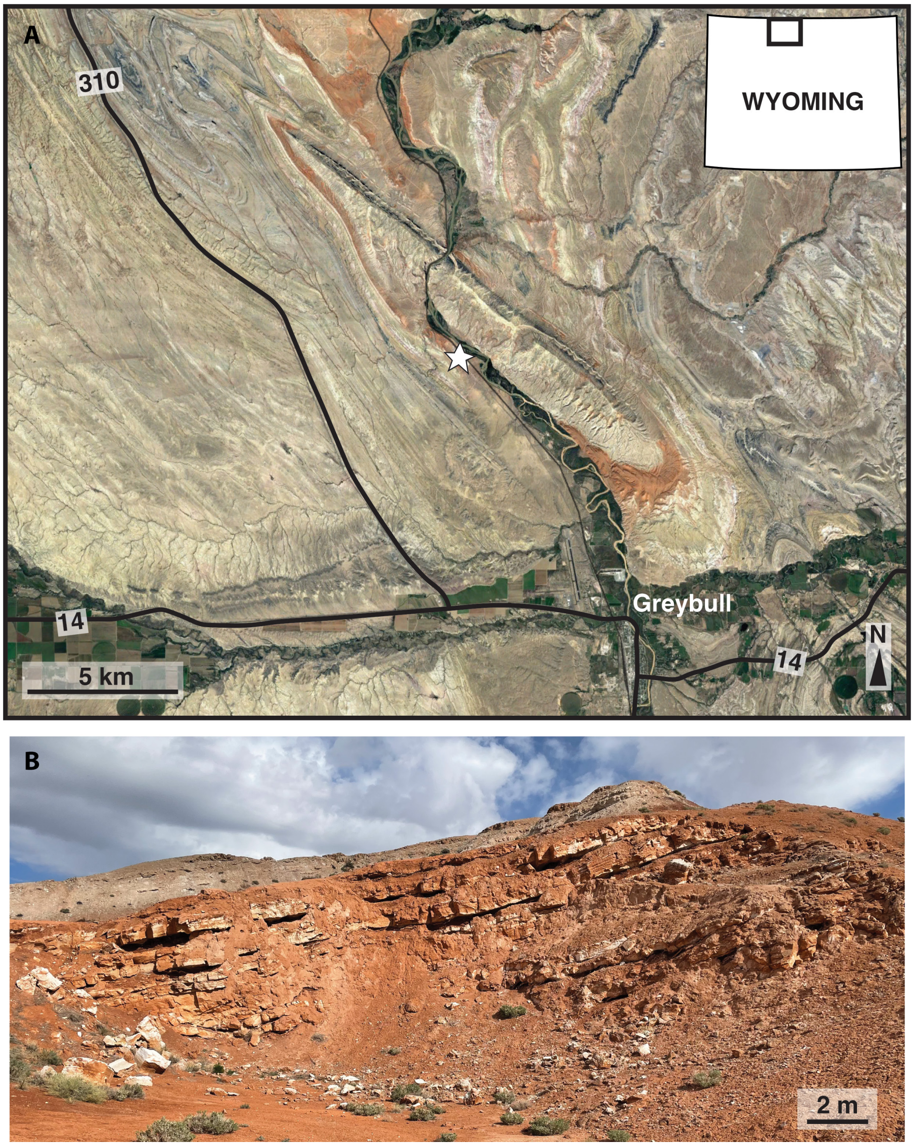

FIGURE 2 Location of study outcrop. (A) Map view of Sheep Mountain Anticline with study site marked by white star. (B) Outcrop consists of alternating units of red mudstone and bedded gypsum.

YR 8/6) on fresh exposures. The most prominent feature of these rocks are beds composed of vertical crystals. The vertical crystals are seen in outcrop and in thin section (Figure 4).

In outcrop, this lithology is characterised by multiple beds of vertically oriented crystals ranging in thickness from *ca* 0.25 to 0.75 cm. In thin section, the vertically oriented crystals are bladed or acicular gypsum (Figure 4B,C). Some crystals are twinned to form a swallowtail shape. The beds have flat bottoms and pointy tops. Thin (*ca* 0.05 cm thick) wavy laminations of gypsum mudstone form the base of some beds of vertical gypsum crystals and drape over their pointy tops (Figure 4B,C). Gypsum mudstone, here, appears in thin section as opaque, mud-sized (less than 0.0625 mm) particles of gypsum; their small size makes it difficult to accurately distinguish crystals from clastic grains. The gypsum mudstone comprises only a small percentage of the bottom-growth gypsum lithology. One 42 cm thick unit (4.56–4.86 m above the base of the outcrop; see Figure 3) consists only of vertically oriented crystals. X-ray diffraction bulk analysis of three samples of this lithology indicated that it is composed of *ca* 97% gypsum and *ca* 3% clay minerals (Table 1). No evidence of anhydrite or carbonate minerals was found in this lithology.

Interpretations

This bedded gypsum lithology, characterised by vertical crystals, is interpreted as bottom-growth gypsum. Bottom-growth gypsum grows upward from the sediment–water interface, precipitating from $CaSO_4$-rich saline surface

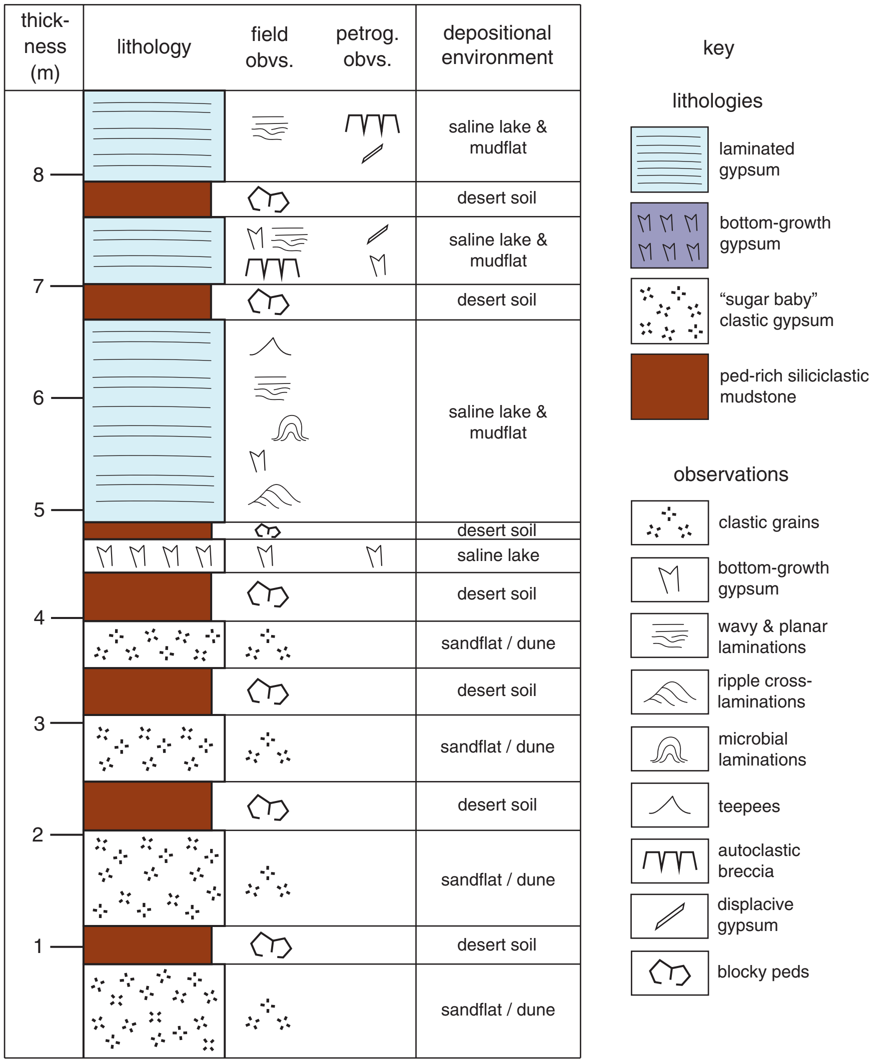

FIGURE 3 Stratigraphic column with field and petrographic observations, lithologies and depositional environment interpretations.

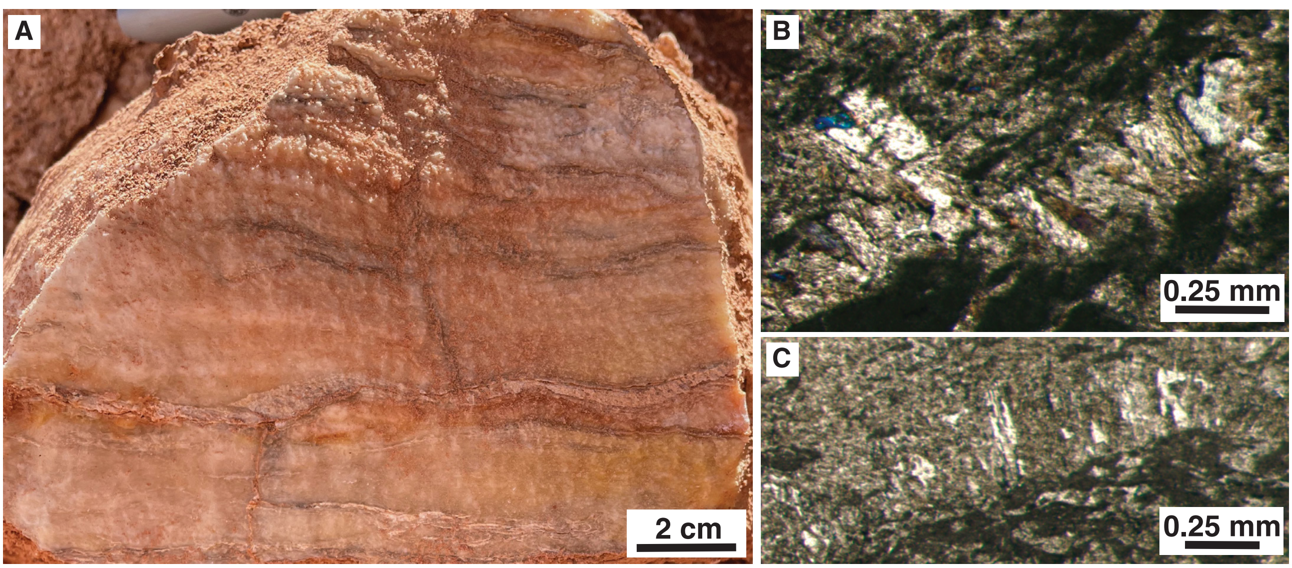

FIGURE 4 Bottom-growth gypsum lithology. (A) Outcrop view showing multiple beds with vertical textures. (B) Thin-section view of bladed and swallowtail-shaped bottom-growth gypsum crystals. (C) Thin-section view of acicular bottom-growth gypsum crystals. The dark material in B and C is gypsum mud.

TABLE 1 X-ray diffraction bulk analysis of laminated gypsum results, expressed in percentages, for bottom-growth gypsum. All three samples were taken from the bottom-growth gypsum unit at 4.56–4.86 m above the base of the outcrop.

Sample ID	Quartz	Dolomite	Gypsum	Anhydrite	Bassanite	Celestine	Total clay	Mixed layer illite/smectite	Illite & mica	Kaolinite	Chlorite	Total
1	1	3.7	93	0	0	0	2.6	0.3	1.9	0.2	0.2	100
2	0.2	1.8	97	0	0	0.4	1.1	0.4	0.5	0.1	0.1	100
3	0.5	1.5	96	0	0	0.2	1.8	1.1	0.5	0.1	0.1	100

waters, including lakes, lagoons and seas. Bottom-growth gypsum forms beds of vertically oriented gypsum crystals that are acicular, bladed or swallowtail shaped (Hardie & Eugster, 1971; Benison et al., 2007).

Bottom-growth gypsum only forms in saline surface waters. The one unit consisting solely of bottom-growth gypsum is both underlain and overlain by red siliciclastic mudstone with abundant peds. In addition, some laminated gypsum units include localised beds of bottom-growth gypsum. The bottom-growth gypsum probably precipitated in situ in saline lakes.

The laminations of gypsum mud that underlie the bottom-growth gypsum beds and drape over their pointy crystal tops may be composed of tiny (sub-millimetre scale) cumulate gypsum crystals, which precipitate in the water column and settle to the bottom. Both bottom-growth and cumulate gypsum crystals may precipitate at the same time from a saline lake. However, these gypsum mud laminations could alternatively be composed of clastic gypsum grains. If the gypsum mud is clastic, it would probably represent reworked gypsum crystals. Deposition of clastic gypsum may occur at the same time, or at a different time, as the precipitation of bottom-growth gypsum crystals. If the gypsum mud is clastic, there are two depositional pathways: (1) dilute floodwaters transport the grains at times alternating with times of evapoconcentration and (2) winds transport and deposit the grains regardless of lake water chemistry. However, the gypsum mud observed in this study is composed of particles too small to evaluate for their origin as either cumulate crystals or clastic grains. Regardless, the bottom-growth gypsum crystals are the dominant component in this lithology and they record chemical precipitation in saline lakes.

4.1.2 | Laminated gypsum lithology: Ephemeral saline lake and saturated mudflat lithofacies

Results

The laminated gypsum lithology is characterised by planar, convolute and crinkly thin and thick laminations of pale grey (GLEY 2 7/1 10B) and pure white gypsum mudstone (Figure 5A,B). Several textures of gypsum were observed, including thin discontinuous beds of vertically oriented gypsum crystals with mud drapes (Figure 5F); crinkly, doming laminations of gypsum mud in the shapes of mounds (Figure 5G); and pointy, tent-shaped laminations and convolute laminations of gypsum mud (Figure 5E). Several syndepositional textures of gypsum are documented from thin section, including randomly oriented acicular gypsum crystals in a gypsum mudstone

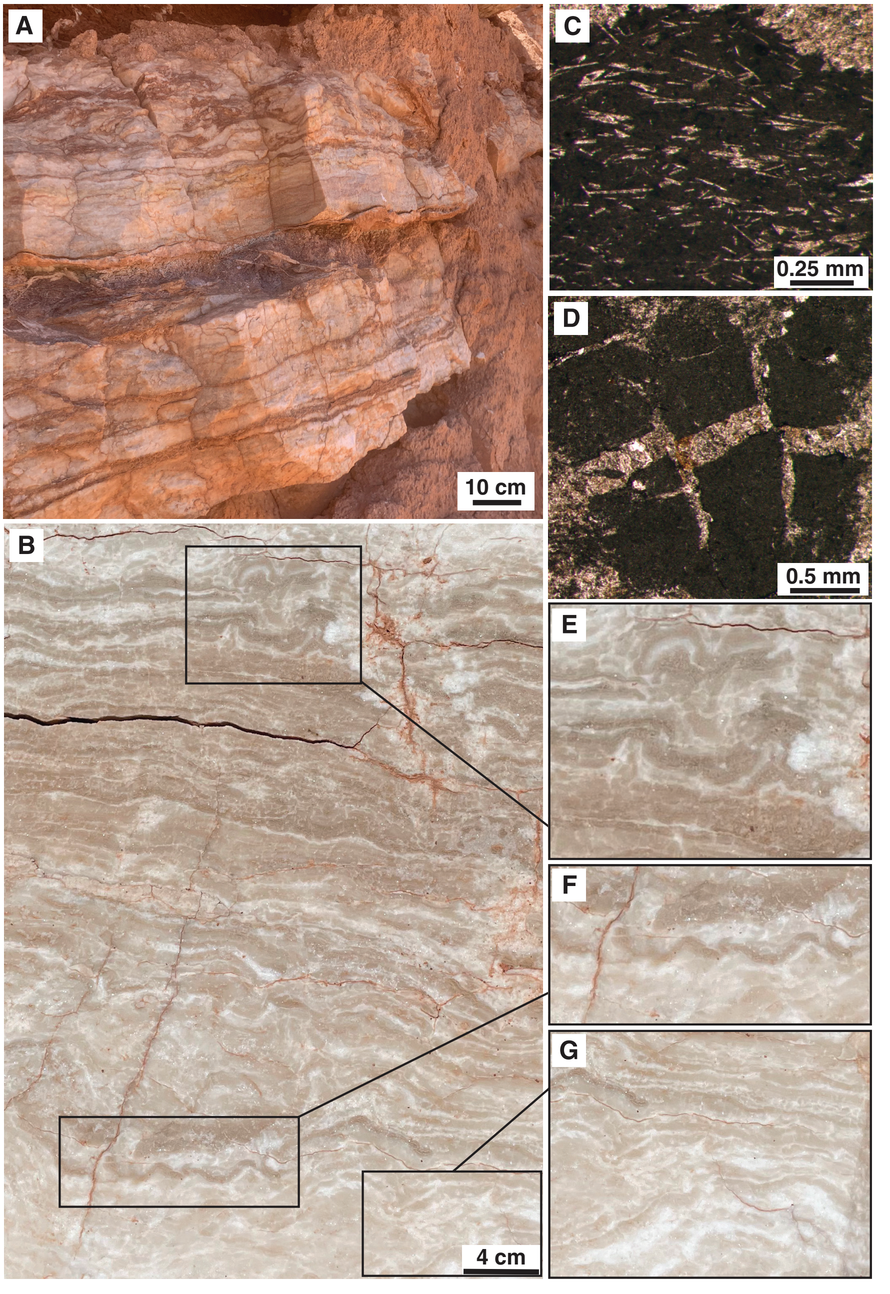

FIGURE 5 Laminated gypsum lithology, as shown in cross-sectional views. All images are shown with respect to stratigraphic up. (A) Resistant gypsum beds with abundant textures. (B) Relatively unweathered fallen block from lowermost laminated gypsum unit (see Figure 3). (C) Thin section view of displacive gypsum. (D) Thin-section view of autoclastic breccia. (E) Teepee structures and convolute laminations. (F) Pointy shapes interpreted as bottom-growth gypsum. (G) Wavy, doming laminations interpreted as microbial mats.

matrix (Figure 5C) and blocks of gypsum mud with vertical cracks (Figure 5D).

There are three units of the laminated gypsum lithology at the study outcrop. The units exist at 4.98–6.77 m, 7.09–7.76 m and 7.91–8.65 m above the base of the outcrop (Figure 3). The units range in thickness from 60 to 82 cm. Laminated gypsum units are interbedded with red siliciclastic mudstones. No evidence of carbonate minerals was found in this lithology.

Interpretations

The majority of this lithology is composed of gypsum mud, for which there are two possible origins: (1) cumulate crystals that precipitated in a surface water body and settled to the bottom and (2) reworked clastic grains. Planar laminations of cumulate gypsum crystals, as well as clastic gypsum mud, form from settling in gypsum-precipitating lakes or from traction or saltation along lake bottoms (Abrantes et al., 2016). Crinkly laminations and dome-shaped laminations of gypsum mud are interpreted to represent microbial mats, which may grow in shallow surface waters (Noffke et al., 2001; Figure 5G). Convolute laminations are products of soft sediment deformation (Figure 5E). Teepee structures, laminations shaped like pointy tents, are products of dewatering after rapid deposition on wet sediment (Figure 5E). Cumulate and/or clastic gypsum mud laminations, with some bottom-growth gypsum, probably formed in shallow saline lakes (Figure 5F).

Several diagenetic textures are also present in the laminated gypsum lithology. When $CaSO_4$-rich groundwaters precipitate gypsum crystals in pore spaces in unconsolidated muds, the resulting texture is acicular gypsum crystals randomly oriented in a mud matrix. This texture is called displacive gypsum and is indicative of saline mudflats adjacent to saline lakes or lagoons (Casas & Lowenstein, 1989; Smoot & Lowenstein, 1991; Benison et al., 2007; Figure 5C). Blocky cracked gypsum mud is interpreted as autoclastic breccia, which is a product of repeated wetting and drying of mud (Goldstein, 1998; Figure 5D).

The sedimentary textures, sedimentary structures and syndepositional-to-early diagenetic features in the laminated gypsum lithology together indicate formation in shallow lakes and saturated mudflats that experienced stages of flooding and desiccation, causing lake levels to fluctuate over short time spans (probably days to years). Displacive crystals and autoclastic breccia in mudstone host rocks indicate mudflats formed after lakes.

4.1.3 | Clastic gypsum lithology: Sandflat/dune lithofacies

Results

The clastic gypsum lithology is dull reddish yellow (5YR 6/6) on weathered surfaces and pure white, vitreous and sugary on fresh surfaces (Figure 6A,B). Local mine workers call this lithology 'sugar baby' due to its pure white colour and fine grain size, resembling sugar. In addition, according to the mine workers, this lithology is pure (>99%) gypsum, making it economically valuable to them. The beds are massive and friable. This lithology has grain

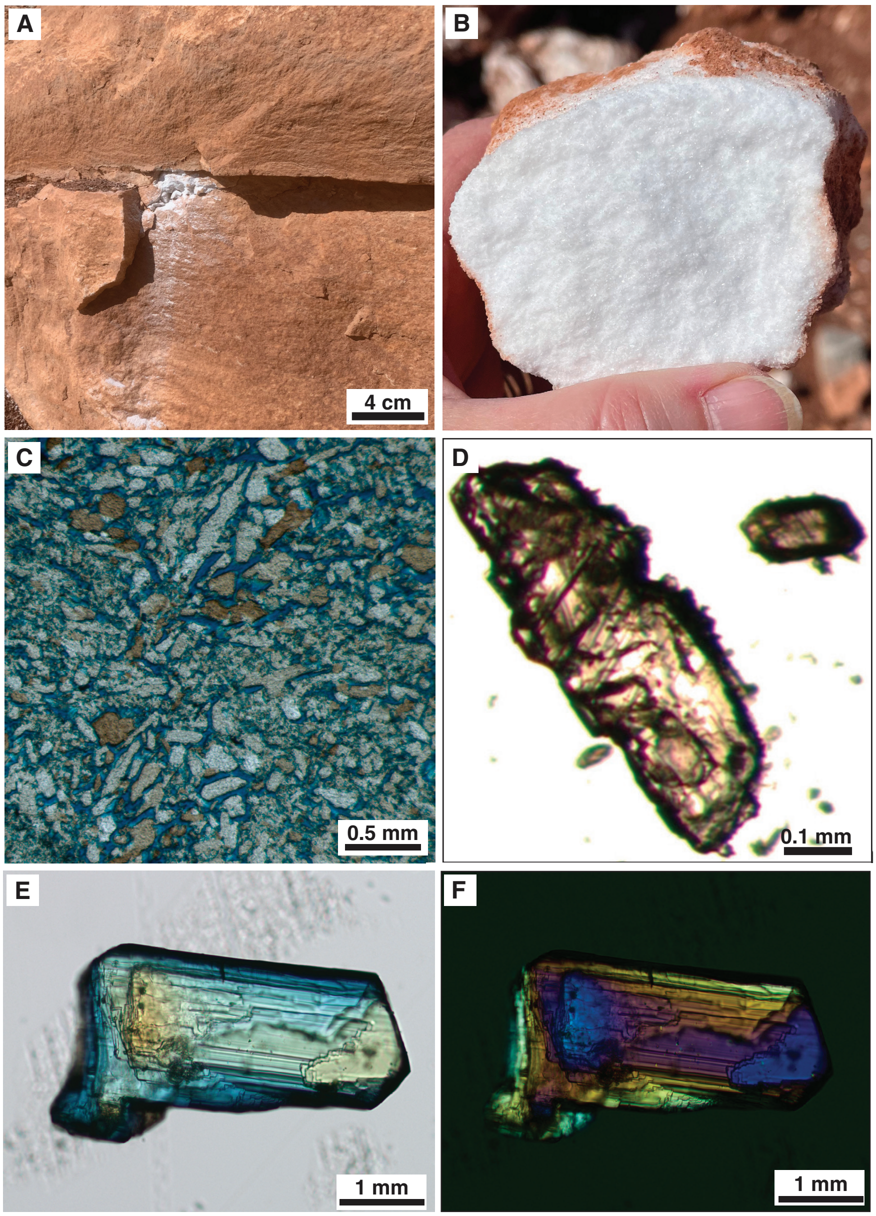

FIGURE 6 Clastic gypsum lithology. (A) Outcrop view shows how weathered surfaces can look like siliciclastic sandstone. (B) White, sugary and vitreous fresh surface. (C) Thin-section view of abraded blade-shaped grains. Blue colour is dyed epoxy. (D) Individual grains shown in magnified view using transmitted light. (E, F) An individual grain shown in partially polarised (E) and cross-polarised light. Note optical continuity.

sizes ranging from coarse sand (1 mm) to very fine sand (0.06 mm); most (>90%) of the grains are fine-medium sand (0.1–0.5 mm; Figure 6D). The grains are bladed or needle-shaped with low sphericity and are subrounded to angular (Figure 6C, D). Grains are randomly oriented and flake off the rock easily. Some grain surfaces have high topographic relief (Figure 6D). Grains flaked from this lithology and viewed under cross-polarised light showed optical continuity (Figure 6E,F).

Analyses of fresh surfaces by a portable XRF in the field detected only calcium and sulphur. Mine workers report that their laboratory analyses confirm this clastic gypsum lithology is composed of pure gypsum. There are four units of this lithology at this outcrop (Figure 3). They are 0–0.95 m, 1.3–2.06 m, 2.5–3.1 m and 3.45–3.98 m above the base of the outcrop. They range in thickness from 53 to 95 cm. As with the other bedded gypsum lithologies, clastic gypsum units are interbedded with red siliciclastic mudstones with abundant peds. No evidence of carbonate minerals was found in this lithology.

Interpretations

Based on the elongated, bladed shape of the grains, their high-relief surface textures and the optical continuity in birefringence, these grains are probably reworked crystals. Furthermore, the sand-size and bladed shape suggest these grains were originally bottom-growth crystals, although a displacive origin is also a possibility for some grains. The grain shapes and surface textures, indicative of abraded crystals, suggest entrainment, transportation and deposition by wind. The clastic gypsum lithology is interpreted as reworked bottom-growth gypsum crystals deposited as clastic grains in sandflats and dunes (Benison et al., 2007; Benison, 2017, 2019a).

The clastic gypsum lithology is interpreted to be an aeolian deposit despite the absence of cross-bedding. High-angle, trough and tangential cross-bedding forms in aeolian deposits of rounded and spherical grains. The extent to which cross-bedding forms and is preserved in deposits of elongated, bladed grains is not yet well-studied. The bladed nature of the gypsum grains that compose the clastic gypsum lithology may account for the lack of cross-bedding.

4.1.4 | Ped-rich siliciclastic mudstone lithology: Desert soil lithofacies

Results

Interbedded with each unit of bedded gypsum is a unit of red (5 YR 4/6) siliciclastic mudstone (Figure 3). Red mudstone units range from 16 to 74 cm in thickness. The units are massive. These red mudstone units are characterised by abundant blocky peds (Figure 7A). Each ped is subrectangular, composed of red mudstone and no more than 2 cm in diameter.

There are randomly oriented, blue-grey (GLEY 2 8/1 5B) patches in the red mudstone (Figure 7A). The red mudstone is riddled with cross-cutting veins filled with fibrous gypsum cement. There are two subcategories of these veins: (1) thin (0.4–0.6 cm wide), subvertical to subhorizontal veins with tapered ends and surrounded by blue-grey halos (Figure 7A), and (2) relatively thick (1–2 cm wide), subhorizontal veins that are not related to the blue-grey colouration.

Interpretations

Blocky peds are the product of wetting and drying of soils (Goldstein, 1998). The randomly oriented blue-grey patches are interpreted to be reduction spots, and may be places where decaying organics, probably roots, reduced iron oxides. All gypsum veins are interpreted to have formed when late-stage saline groundwaters precipitated fibrous gypsum cement in cracks. The thin veins with blue-grey halos probably originated as roots, as suggested by the veins' tapered ends (Figure 7A). Based on the blocky peds, root features and localised reduction zones, the ped-rich siliciclastic mudstone is interpreted to represent a desert palaeosol.

4.2 | Summary of interpreted depositional environments

The study section of the Red Peak Formation is composed of alternating units of bedded gypsum and red palaeosols (Figures 2 and 3). There are three distinct lithologies of the bedded gypsum: bottom-growth gypsum, laminated gypsum and clastic gypsum. At the bottom of the section, the bedded gypsum is clastic (Figure 3). It is interpreted as aeolian sandflat and dune deposits composed of reworked bottom-growth gypsum material. In the middle of the section, there is one unit of bottom-growth gypsum. The uppermost bedded gypsum units are composed of laminated gypsum (Figure 3). This outcrop of the Red Peak Formation was formed in shallow saline lakes and associated mudflats, sandflats, dunes and desert soils.

Because the succession of vertically adjacent lithologies in the Red Peak Formation represents laterally adjacent facies documented in modern saline lake systems, the stratigraphic sequence follows Walther's Law (Middleton, 1973). In other words, the lithologies in the Red Peak Formation formed in depositional environments that may have co-existed at the same time. The stratigraphic succession of deposits at this outcrop probably

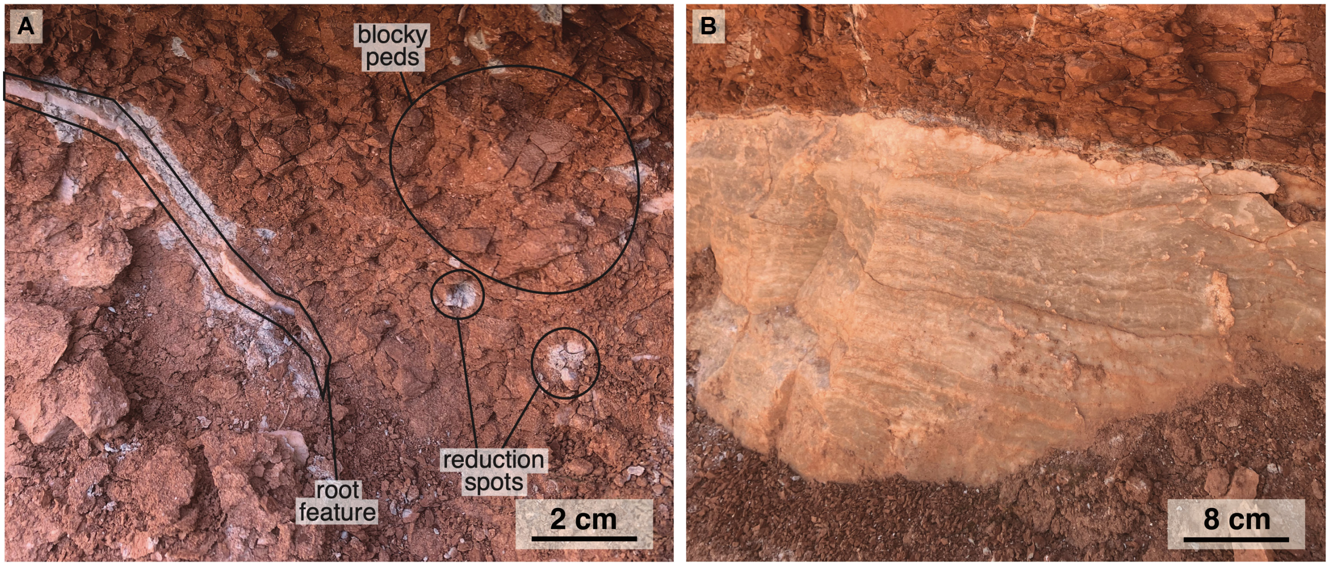

FIGURE 7 Ped-rich mudstone lithology. (A) Annotated outcrop view showing blocky peds, reduction spots and root features filled with gypsum cement. (B) Outcrop view of stratigraphic contacts of red mudstone with a laminated gypsum unit.

results from the migration of subenvironments due to fluctuating saline lake levels and groundwaters, topography and winds. This suggests that there were no major interruptions in sedimentation or major changes in climate over the time of formation of the outcrop.

The lithologies and textures described from this study fit well with the model for shallow saline lakes and associated environments (Lowenstein & Hardie, 1985; Benison et al., 2007; Benison, 2017, 2019a; Figure 8). Bottom-growth gypsum represents the chemical precipitation of gypsum during the evapoconcentration stages of a $CaSO_4$-rich lake. The laminated gypsum represents chemical precipitation, physical reworking and some microbial influence of gypsum in both the lake and adjacent mudflats. Shallow saline groundwaters are an additional source of gypsum, responsible for displacive gypsum crystals. Another possible source of gypsum may have been efflorescent crusts, which are beds containing tiny (submillimetre) salt crystals on desiccated lake surfaces; while textures indicative of remnant efflorescent crusts were not observed, they are rarely preserved as they are vulnerable to wind erosion (Smoot & Castens-Seidell, 1994; Benison & Goldstein, 2000; Benison et al., 2007). The sediments of these lakes and mudflats underwent wetting and drying, driven by fluctuations of the saline groundwater table (Figure 9). The clastic gypsum units, in association with abundant red palaeosols and wetting-drying features, suggest that the saline lakes were, at times, ephemeral. Another important process in these shallow saline lake systems was recycling by wind, as subaerial sediments of mudflats and desiccated lakes would have been vulnerable in these subaerial environments. Wind entrained, abraded, sorted and deposited the bottom-growth and other gypsum crystals as clastic grains in nearby sandflats and dunes.

Southern Western Australia contains shallow saline lakes, mudflats, sandflats, dunes and red desert soils and serves as a modern analogue for the Red Peak Formation (Benison et al., 2007). These modern lakes precipitate halite and gypsum and are surrounded by reworked gypsum and red siliciclastics. Flooding, evapoconcentration and desiccation cycles are dynamic and cause fluctuation of the saline groundwater table, lake levels and lake compositions. Winds are also an important component of these Western Australian systems, causing reworking of the saline minerals (Benison & Bowen, 2013).

4.3 | Diagenetic sequence of events

The most distinct diagenetic textures observed in the Red Peak Formation are seen in the laminated gypsum lithology and the ped-rich mudstone lithology. In the laminated gypsum lithology, there is abundant displacive gypsum, which forms relatively early from $CaSO_4$-rich groundwaters just centimetres below the surface in saturated mudflats. In addition, blocky, vertically cracked gypsum mudstone within this lithology probably formed as autoclastic breccia, a product of wetting and drying (Goldstein, 1998). The ped-rich red mudstone lithology is characterised by blocky peds, reduction spots and cross-cutting gypsum veins. Fibrous gypsum veins were probably the last diagenetic feature to form, as evidenced by cross-cutting relationships showing fractures post-dated

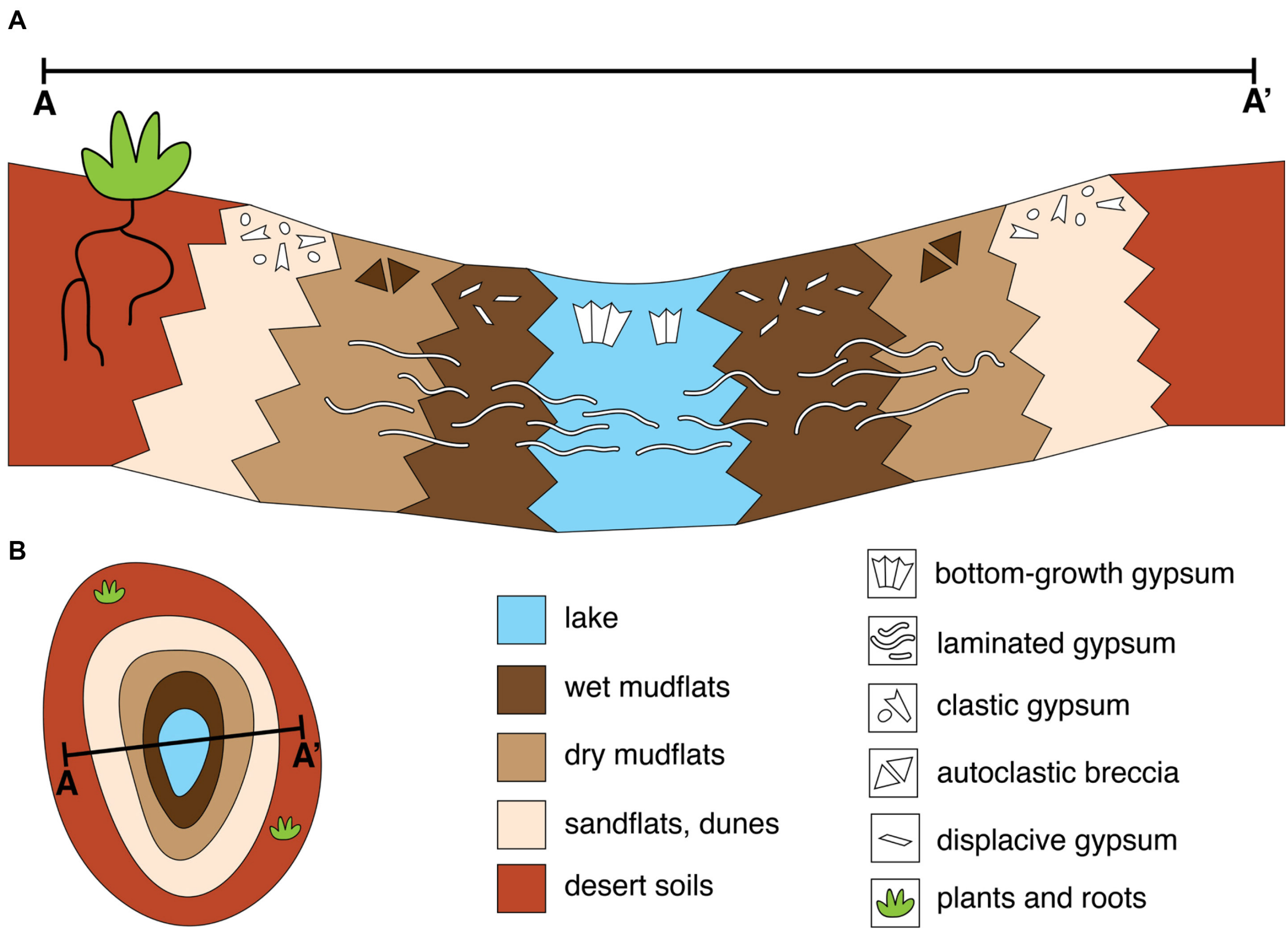

FIGURE 8 Depositional model for the Triassic Red Peak Formation. (A) Idealised cross-sectional view showing subenvironments and their dominant lithologies and syndepositional features. (B) Idealised map view. Note that A–A′ correspond to A–A′ in panel A. Note that this model depicts the lake at only one stage.

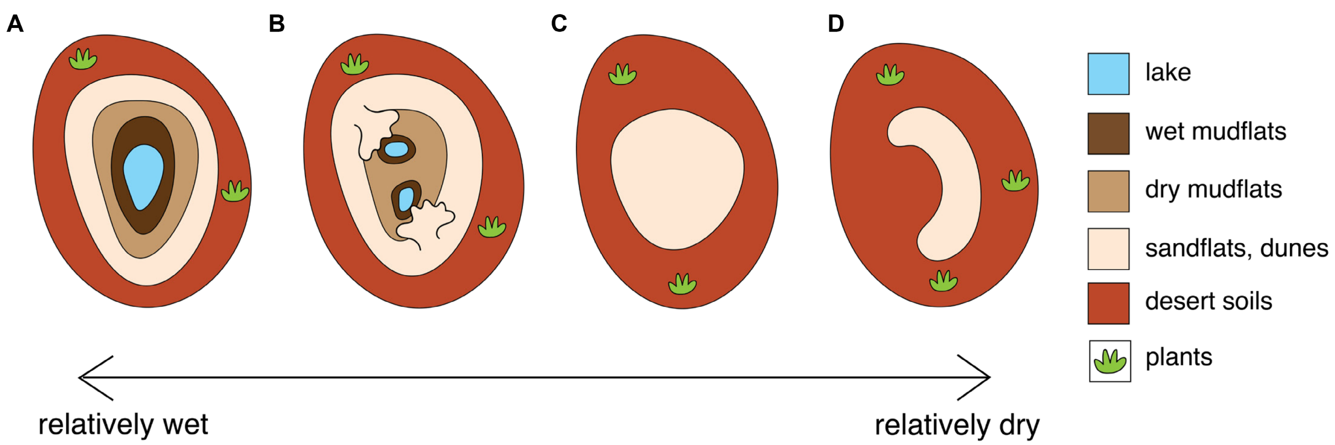

FIGURE 9 Schematic model of map views depicting various stages of evapoconcentration and desiccation in the Red Peak lake systems. (A) Evapoconcentration stage includes saline lake. (B) Advanced evapoconcentration stage. (C) Desiccation stage. (D) Advanced desiccation stage dominated by aeolian bedforms and soils. Return to evapoconcentration stage depicted in panel A could have occurred by precipitation and flooding events and/or by rising groundwater table.

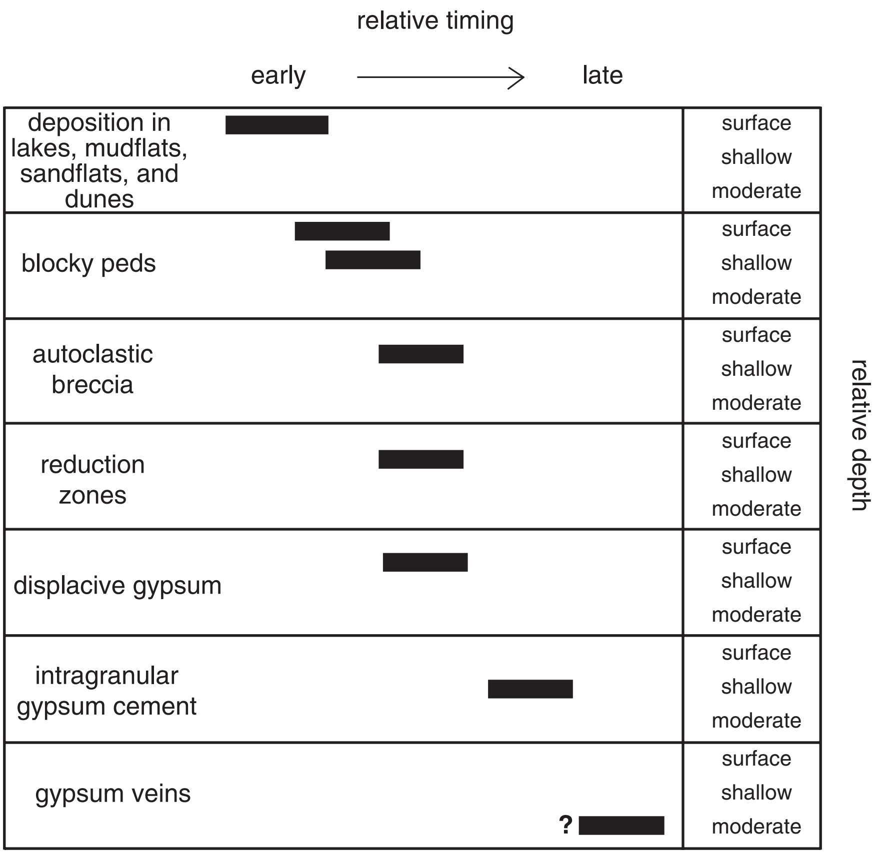

FIGURE 10 Paragenetic sequence of the Red Peak Formation based on observations made in this study. Note relative timing is shown by lateral relationships of black bars. Vertical placement of black bars indicates surface, shallow depth and moderate depth of process.

rock cementation (Holliday, 1970). No evidence of deep burial of these rocks, including close grain contacts or other compaction features, was observed. Figure 10 shows the paragenetic sequence interpreted for this outcrop of the Red Peak Formation.

5 | DISCUSSION

5.1 | Textures in ancient gypsum

This study describes textures and interprets depositional environments from bedded gypsum that is approximately 240 Myr old. Most previous studies that include textural descriptions of well-preserved gypsum have focussed on Miocene rocks of the Mediterranean region (Attia et al., 1995; Manzi, et al., 2009; Lugli, et al., 2010; Dela Pierre et al., 2011). It is remarkable that the Triassic Red Peak Formation gypsum is well-preserved and appears relatively unaltered by heat, pressure and subsurface waters. This shows that ancient gypsum can reveal depositional conditions through detailed observations of its textures. Additionally, petrographic documentation of such unaltered gypsum shows the promise for future fluid inclusion studies to yield specific environmental indicators such as surface water temperature, composition and microbiology (Benison et al., 1998; Benison & Goldstein, 1999; Zambito & Benison, 2013).

Textures of ancient gypsum have generally been overlooked in depositional studies. For much of the ancient gypsum that has been observed, it is commonly altered. Gypsum and its dehydrated form anhydrite are vulnerable to polymorphic transition, that is, they undergo dehydration and rehydration. Therefore, to the current knowledge, most ancient gypsum known is in the form of anhydrite; depositional textures have been altered or lost. Another form of alteration is the replacement of gypsum and/or anhydrite by other minerals such as halite (Andeskie et al., 2018). This process also overwrites depositional textures. In contrast, the bedded gypsum in the Triassic Red Peak Formation described in this study is remarkable in its preservation; there is no petrographic or mineralogical evidence that this gypsum experienced diagenetic alteration. In particular, there is no anhydrite or interlocking crystal mosaic (Table 1). In addition, the clastic gypsum grains are optically continuous, suggesting original gypsum composition has not been altered (Figure 6E,F). The results of this study emphasise the potential for ancient bedded gypsum to maintain original depositional textures and primary fluid inclusions, allowing for interpretations of past environments, climates and life.

FIGURE 11 The approximate locations and general descriptions of the Red Peak Formation and other Permo-Triassic stratigraphic units composed of red beds and bedded evaporites. (A) Palaeogeographical map of Pangea 240 Ma (modified from Blakey & Ranney, 2018). (B) Relevant stratigraphic units with descriptions and interpretations.

A

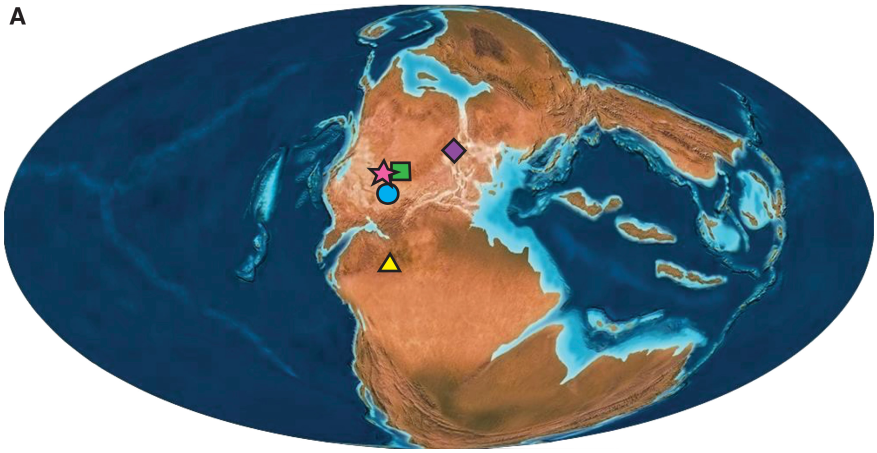

B

formation	outcrop	core	lithologies	depositional environments
Permian Nippewalla Group *Benison et al. 1998* *Benison and Goldstein 2001,* *Zambito and Benison 2013,* *Sweet et al. 2013,* *Foster et al. 2014,* *Benison et al. 2015*	X	X	bedded halite, bedded gypsum, displacive halite, displacive gypsum, red mudstone, red sandstone	shallow saline lakes, mudflats, sandflats, dunes, desert soils
Permian Opeche Shale + Minnekhata Limestone *Benison et al. 1998* *Benison and Goldstein 2000,* *Benison et al. 2018*	X	X	bedded halite, displacive halite, red mudstone, rare bedded gypsum	shallow saline lakes, mudflats, desert soils
Triassic Mercia Mudstone Group *Andeskie et al. 2018*	X	X	bedded halite, displacive halite, red mudstone	shallow saline lakes, mudflats, desert soils
Permian-Triassic Motuca Formation *Abrantes et al. 2016*	X		bedded gypsum, red mudstone	shallow saline lakes, mudflats
Triassic Red Peak Formation *This study*	X		bedded gypsum, displacive gypsum, red mudstone	shallow saline lakes, mudflats, sandflats, desert soils

5.2 | Comparison with other Permo-Triassic red beds and bedded evaporites

The Red Peak Formation is atypical due to the relatively uncommon association of red beds and bedded evaporites in the rock record. The Red Peak Formation is similar in age and lithology to bedded gypsum and associated red beds from the Permian and Triassic of Kansas and Oklahoma, North Dakota and South Dakota, Northern Ireland and northern Brazil. Figure 11 shows the approximate palaeogeographical locations of these rocks and their interpreted environments on Pangea.

The Permian Nippewalla Group from Kansas and Oklahoma consists of bedded halite, bedded gypsum, displacive halite, displacive gypsum, and red mudstones and red sandstones that probably formed in extremely acid saline lakes, mudflats, sandflats, dunes and desert soils (Benison et al., 1998; Benison & Goldstein, 2001; Sweet et al., 2013; Zambito & Benison, 2013; Foster et al., 2014; Benison et al., 2015; Petras, 2021). Like the Red Peak Formation, the Nippewalla Group has bottom-growth gypsum and laminated gypsum. In contrast to the Red Peak Formation, the Nippewalla Group bedded gypsum has largely been replaced by anhydrite. As a result, the crystals are blocky and fine detail has been lost.

The Permian Opeche Shale from North Dakota and South Dakota consists of bedded and displacive halite and red fine-grained siliciclastics that together represent an acid saline lake system and red desert soils (Benison & Goldstein, 2000). The Opeche Shale contains rare bedded gypsum, unlike the Red Peak Formation, which contains abundant bedded gypsum. The red mudstone of the Opeche Shale is characterised by palaeosol features including blocky peds and root features. The red mudstone of the Red Peak Formation is similarly characterised by blocky peds and root features and is interpreted as a desert palaeosol.

The Triassic Mercia Mudstone Group from Northern Ireland is interpreted to have formed in shallow saline lakes, saline mudflats, dry mudflats and desert soils (Andeskie et al., 2018). These environments are also represented in the Red Peak Formation. However, the Mercia Mudstone contains abundant halite, including bedded halite, displacive halite and replacement halite after gypsum. The Mercia Mudstone contains beds of halite in the form of swallowtail bottom-growth gypsum crystal shapes. In contrast, the bottom-growth gypsum in the Red Peak Formation retains its original composition.

The Permo-Triassic Motuca Formation from northern Brazil is also composed of red siliciclastic mudstones and bedded gypsum (Abrantes et al., 2016). Lithologies of the bedded gypsum include laminated gypsum and clastic gypsum. The laminated gypsum is characterised by planar to wavy thick and thin laminations of white and grey gypsum mudstone and is interpreted as shallow saline lake deposits. The clastic gypsum is called "gypsarenite" and is interpreted as gypsum crystals reworked in subaqueous conditions. The laminated bedded gypsum of the Motuca Formation is very similar to the laminated gypsum of the Red Peak Formation. However, the gypsum of the Motuca Formation probably underwent dehydration to anhydrite, and was later rehydrated back to gypsum (Abrantes et al., 2016).

The Red Peak Formation is similar to other Permo-Triassic red bed and evaporite deposits from Pangea in that all are composed of fine-grained red bed siliciclastics and bedded evaporites that formed in continental saline settings. Carbonate minerals are rare in these rocks, and when present, are a replacement phase of gypsum (Benison et al., 2018). Signs of life are uncommon and include root traces and rare suspect insect burrows (Zambito et al., 2012). Microorganisms have been found in fluid inclusions in bedded halite (Benison, 2019b; Gibson & Benison, 2023). This assemblage of Permo-Triassic units is lithologically equivalent and generally time equivalent across Pangea. Placing temporal constraints on these rocks is challenging for several reasons. Minerals useful for absolute geochronology are absent in these rocks. The ages of these rocks are mainly understood with relative dating methods; they are underlain by strata containing early Permian fossils and overlain by strata containing Jurassic fossils (Zambito et al., 2012). The only absolute date from these rocks comes from the identification of the Kaiman Superchron recorded in iron-oxide minerals; this places a 267 Myr age in the Dog Creek Shale, the uppermost formation of the Nippewalla Group of Kansas (Foster et al., 2014).

Unlike most previous studies of Permo-Triassic evaporites, which described detailed sedimentological evidence from subsurface cores, or subsurface mine walls, and outcrops, this study of the Red Peak Formation relies solely on evidence preserved in outcrop. While similar in depositional interpretations, the Red Peak Formation is different from other comparable deposits in its well-preserved gypsum composition and texture. The fact that the bedded gypsum units of the Red Peak Formation are composed almost entirely of gypsum and no anhydrite means that the Red Peak Formation did not undergo heating or deformation to the extent needed to remove the waters from the calcium sulphate or chemically replace the gypsum. The unusual preservation of this ancient gypsum indicates that it did not undergo dehydration to anhydrite and has remained unaltered through time.

5.2.1 | Was there ever halite in the Red Peak Formation?

Bedded evaporites in the Red Peak Formation are composed of gypsum and contain no evidence of halite. However, halite is a major component of other Permo-Triassic red beds and evaporites. Possible explanations for this absence of halite are: (1) halite never existed in this system, (2) ephemeral halite existed in the system but was not preserved or (3) halite existed in this system but was dissolved by later diagenesis.

It is possible that the gypsum-precipitating lakes and groundwaters of the Red Peak Formation never precipitated a significant amount of halite. In modern analogues from Western Australia, lakes primarily precipitate either gypsum or halite. Lakes that are dominated by one salt mineral only precipitate a minor amount of the other; most lakes are either gypsum-rich with minor halite or halite-rich with minor gypsum (Benison et al., 2007).

Flooding can dissolve halite in the depositional environment and, therefore, it may not preserve in the subsurface; the long-term subsurface record of some modern halite-rich lakes is actually poor in, or absent of, halite. The semi-arid climate in southern Western Australia allows for enough rain to sometimes dissolve surface and shallow subsurface halite. Here, halite is only retained for short periods of time (months to decades).

Another possibility is that halite formed and was preserved (in the short term) in the Red Peak Formation system but was dissolved during late-stage diagenesis. Halite is more susceptible to dissolution than gypsum. The Permian Nippewalla Group, which is halite-rich in core, lacks halite in outcrop (Benison et al., 2015). However, textures indicative of halite that was later dissolved or altered, such as halite casts and pseudomorphs, were not observed in this study of the Red Peak Formation, as they were in the Nippewalla Group.

Based upon the information currently known, it is not possible to distinguish between these three hypotheses about the presence or lack of halite in the depositional environments of the Red Peak Formation. The presence of bedded halite in any well-preserved cores of the Red Peak Formation from moderate depths would suggest the third hypothesis that halite was present and persistent in the depositional environment but dissolved by late-stage diagenesis. Additional observations of halite casts or moulds in nearby outcrops of the Red Peak Formation would also suggest the third hypothesis. Regardless of whether halite was ever present, the bedded gypsum and red beds of the Red Peak Formation record an acid-saline lake and groundwater system.

5.2.2 | Were lakes and groundwaters of the Red Peak Formation acidic?

Late Permian and early Triassic red beds and bedded evaporites were probably formed in acid lake and groundwater systems (Benison et al., 1998; Benison & Goldstein, 2002; Eichenlaub, 2016; Eichenlaub et al., 2016; Andeskie et al., 2018). Raman spectroscopy of fluid inclusions in halite in the Permian Nippewalla Group shows single bisulphate peaks, indicating a pH less than 2. Two bisulphate peaks present in Raman spectra in halite from the Permian Opeche Shale documented pH less than 0 (Benison et al., 1998). Although this current study did not employ Raman spectroscopy, there are other indicators that the early Triassic lake waters and groundwaters of Wyoming were probably acid. The Red Peak Formation contains an abundance of gypsum and iron oxides and a paucity of carbonates, which together are characteristic of acid brine systems (Benison & Goldstein, 2002). Where there are isolated thin carbonate units in Permo-Triassic red bed and evaporite successions, they have remnant gypsum and textural characteristics of neomorphism, suggesting that the carbonate phase is a diagenetic replacement phase after gypsum (Benison et al., 2018). For these reasons, the Red Peak Formation may have been an acid saline lake and groundwater system.

5.2.3 | A long-lived regional acid saline system

The best known modern analogue for Permo-Triassic acid saline lake and groundwater systems are those in southern Western Australia. There, ephemeral lakes have pHs as low as 1.4, salinities as high as 32% total dissolved solids (*ca* 9.5× saltier than modern sea water) and complex chemical composition, with high concentrations of Na, Cl, Ca, Mg, SO_4, Al, Fe and Si, as well as many elevated trace metals (Benison et al., 2007; Benison & Bowen, 2009; Kipnis et al., 2020). Water and air temperatures range from 3 to 50°C. These dynamic systems flood, evapoconcentrate and desiccate over short time spans of days to months. Life is restricted mainly to extremophile microorganisms in the lakes and groundwaters and depauperate flora on soils and dunes.

The Permo-Triassic acid saline lake systems were even more extreme than the modern settings in Western Australia in terms of water chemistry, including acidity, weather and climate, and perhaps life. The bedded halite in the Permian Opeche Shale precipitated from lake waters with pH less than one and some less than zero (Benison et al., 1998). In addition, Opeche and Nippewalla lake waters had high concentrations of Al, Si and Fe (Benison & Goldstein, 2002; Andeskie et al., 2018).

Weather and climate during the Permo-Triassic deposition of acid saline lake and groundwater systems were hotter and drier than modern-day southern Western Australia. Zambito and Benison (2013) documented shallow water temperatures and corresponding localised air temperatures as high as 74°C. Additionally, a maximum diurnal temperature range of 30°C was recorded for the Nippewalla Group, indicating extreme aridity (Zambito & Benison, 2013). In modern Western Australia, bedded halite is ephemeral, forming in lakes during evapoconcentration but dissolving during sheet floods. So, halite is not preserved in the recent rock record there. In contrast, there is abundant Permo-Triassic bedded halite with evidence of flooding, evaporation and desiccation cycles, suggesting that the Permo-Triassic of Pangea was more arid than the semi-arid climate of modern Western Australia.

Western Australia acid saline systems are characterised by both low species diversity and low species abundance (Benison, 2008). Lakes and groundwaters host a community of microorganisms, most of which are acidohalophilic archaea, bacteria, algae and fungi (Mormile et al., 2009; Zaikova et al., 2018). Plants around acid saline lakes in Western Australia are mainly ruby salt brush and a limited number of eucalypts (Benison, 2008; Sanchez Botero et al., 2021). Permo-Triassic red beds and evaporites also have evidence of lake microbes and sparse local vegetation. However, no systematic studies of this life have been conducted. Therefore, it is difficult to compare modern and Permo-Triassic ecosystems.

This study of the Triassic Red Peak Formation of Wyoming adds to our understanding of what seems to be a long-lived, regional system consisting of shallow acid saline lakes surrounded by mudflats, sandflats, dunes and desert soils that existed in equatorial Pangea during the late Permian and early Triassic. These may represent some of the most extreme environments, climates and ecosystems of the Phanerozoic. The textural data and detailed depositional interpretations of bedded gypsum in the Triassic Red Peak Formation will further refine knowledge of the temporal and regional extents of these extreme continental systems of Pangea.

6 | CONCLUSIONS

The Red Peak Formation in north-central Wyoming is characterised by the alternating units of red bed siliciclastics and bedded gypsum. Although the Red Peak Formation makes up most of the well-known Chugwater Group, the bedded gypsums of the Red Peak Formation had not yet been described. Detailed sedimentology of the bedded gypsums from one outcrop of the Red Peak Formation showed three distinct lithologies of bedded gypsum, with three different implications for depositional environment. These bedded gypsums are interbedded with red mudstones that are interpreted to be palaeosols. The association of the bedded gypsum units with palaeosol units strongly suggests a continental origin for the bedded gypsum. The bedded gypsum lithologies are bottom-growth gypsum, laminated gypsum and clastic gypsum. The bottom-growth gypsum is characterised by a vertical texture from multiple beds of bottom-growth gypsum crystals and formed in the bottoms of shallow saline lakes. The laminated gypsum is characterised by planar, convolute and wrinkly laminations of gypsum mudstone and formed in shallow saline lakes and saturated mudflats. The clastic gypsum is composed of bladed and abraded gypsum grains and formed in sandflats and possibly dunes near gypsum-precipitating lakes. This outcrop of the Red Peak Formation in north-central Wyoming formed in shallow acid saline lakes and associated mudflats, sandflats, dunes and desert soils.

Similar continental acid saline environments have been described from the Permian of South Dakota, Oklahoma and Kansas, and the Triassic of Northern Ireland and northern Brazil (Benison et al., 1998; Benison & Goldstein, 2000; Abrantes et al., 2016; Andeskie et al., 2018; Andeskie & Benison, 2020). Ephemeral gypsum-precipitating lakes in Western Australia, which are surrounded by reworked gypsum material in mudflats, sandflats and dunes, and further surrounded by red desert soils, are modern analogues for these Permo-Triassic environments. This study adds another example of an acid saline environment in western equatorial Pangea during Permo-Triassic time and increases our understanding of the extent and longevity of these continental acid-saline systems. A remarkable characteristic of the Red Peak Formation is the original gypsum which may represent some of the oldest unaltered sulphate minerals in the rock record.

ACKNOWLEDGEMENTS

This work was undertaken as part of the M.S. thesis in Geology of MYB. The Georgia-Pacific Gypsum mine in Lovell, Wyoming, is thanked for permission to access and sample rocks. Brigette Petras assisted in the field. Jonathan Knapp suggested this field area and provided assistance in the field, including field-based XRF analysis. James Talbot of K-T Geoservices, Inc., performed X-ray diffraction analyses. James Lamsdell and Amy Weislogel are thanked for reviewing an early draft of this manuscript. This research was partially funded by an Edwin D. McKee Grant from the SEPM Rocky Mountain Section and a West Virginia University Geology Student Field Experience Fund grant to MYB. This paper benefitted from the comments of an anonymous reviewer, associate editor Benjamin F. Walter, and editor-in-chief Peter Swart.

DATA AVAILABILITY STATEMENT

All data and materials used in this study are archived in the Department of Geology and Geography at West Virginia University. Data are also stored in the Research Repository @ WVU, an open access digital repository for the collection, management, preservation and dissemination of intellectual works produced at West Virginia University.

ORCID

Kathleen C. Benison https://orcid.org/0000-0001-6104-2333

REFERENCES

Abrantes, F.R., Nogueira, A.C.R. & Soares, J.L. (2016) Permian paleogeography of west-central Pangea: reconstruction using sabkha-type gypsum-bearing deposits of Parnaiba Basin, Northern Brazil. *Sedimentary Geology*, 341, 175–188.

Andeskie, A.S. & Benison, K.C. (2020) Using sedimentology to address the marine or continental origin of the Permian Hutchinson Salt Member of Kansas. *Sedimentology*, 67, 882–896.

Andeskie, A.S., Benison, K.C., Eichenlaub, L.A. & Raine, R. (2018) Acid-saline-lake systems of the Triassic Mercia Mudstone

Group of County Antrim, Northern Ireland. *Journal of Sedimentary Research*, 88, 385–398.

Attia, O.E., Lowenstein, T.K. & Wali, A. (1995) Middle Miocene gypsum, Gulf of Suez; marine or nonmarine? *Journal of Sedimentary Research*, 65(4), 614–626.

Benison, K.C. (2019a) The physical and chemical sedimentology of two high-altitude acid salars in Chile: sedimentary processes in an extreme environment. *Journal of Sedimentary Research*, 89(2), 147–167.

Benison, K.C. (2019b) How to search for life in Martian chemical sediments and their fluid and solid inclusions using petrographic and spectroscopic methods. *Frontiers in Environmental Science*, 19(108), 1–15.

Benison, K.C. (2017) Gypsum gravel devils in Chile: movement of largest natural grains by wind? *Geology*, 45, 423–426.

Benison, K.C. (2008) Life and death around acid-saline lakes. *Palaios*, 23(9), 571–573.

Benison, K.C. (1997) Field descriptions of sedimentary and diagenetic features in red beds and evaporites of the Nippewalla Group (Middle Permian), Kansas and Oklahoma. *Kansas Geological Survey Open File Report*, 97-21, 63.

Benison, K.C. & Bowen, B.B. (2009) Geochemical characteristics of naturally acid and alkaline saline lakes in southern Western Australia. *Applied Geochemistry*, 24, 268–284.

Benison, K.C. & Bowen, B.B. (2013) Extreme sulfur-cycling in acid brine lake environments of Western Australia. *Chemical Geology*, 251, 154–167.

Benison, K.C. & Bowen, B.B. (2015) The evolution of end-member continental waters: the origin of acidity in southern Western Australia. *GSA Today*, 25(6), 4–10.

Benison, K.C. & Goldstein, R.H. (2002) Recognizing acid lakes and groundwaters in the rock record. *Sedimentary Geology*, 151, 177–185.

Benison, K.C. & Goldstein, R.H. (2001) Evaporites and siliciclastics of the Permian Nippewalla Group, Kansas and Oklahoma: a case for nonmarine deposition. *Sedimentology*, 48, 165–188.

Benison, K.C. & Goldstein, R.H. (2000) Sedimentology of ancient saline pans: an example from the Permian Opeche Shale, Williston Basin, North Dakota. *Journal of Sedimentary Research*, 70, 159–169.

Benison, K.C. & Goldstein, R.H. (1999) Permian paleoclimate data from fluid inclusions in halite. *Chemical Geology*, 154, 113–132.

Benison, K.C., Knapp, J.P., DiFrisco, A.J. & Rasbury, E.T. (2018) The Permian Minnekahta Limestone: a saline lake gypsum replaced by calcite. *The Mountain Geologist*, 55, 59–73.

Benison, K.C., Zambito, J.J. & Knapp, J. (2015) Contrasting siliciclastic-evaporite strata in subsurface and outcrop: an example from the Permian Nippewalla Group of Kansas, USA. *Journal of Sedimentary Research*, 85, 636–645.

Benison, K.C., Bowen, B.B., Oboh-Ikuenobe, F.E., Jagniecki, E.A., LaClair, D.A., Story, S.L., Mormile, M.R. & Hong, B.Y. (2007) Sedimentology of acid saline lakes in southern Western Australia: newly described processes and products of an extreme environment. *Journal of Sedimentary Research*, 77(5), 366–388.

Benison, K.C., Goldstein, R.H., Wopenka, B., Burruss, R.C. & Pasteris, J.D. (1998) Extremely acid Permian lakes and groundwaters in North America. *Nature*, 392, 911–914.

Blakey, R.C. & Ranney, W.D. (2018) *Ancient landscapes of Western North America*. Cham, Switzerland: Springer, p. 228.

Branson, E.B. (1915) Origin of the red beds of western Wyoming. *GSA Bulletin*, 26(1), 217–230.

Casas, E. & Lowenstein, T.K. (1989) Diagenesis of saline pan halite; comparison of petrographic features of modern, Quaternary and Permian halites. *Journal of Sedimentary Research*, 59(5), 724–739.

Cavaroc, V.V. & Flores, R.M. (1917) Red beds of the Triassic Chugwater Group, southwestern Powder River Basin, Wyoming. USGS Survey Bulletin 1917 Evolution of Sedimentary Basins—Powder River Basin, E1–E17.

Dela Pierre, F., Bernardi, E., Cavagna, S., Pierangelo, C., Rocco, G., Irace, A., Lozar, F., Lugli, S., Manzi, V., Natalicchio, M., Roveri, M. & Violanti, D. (2011) The record of the Messinian salinity crisis in the Tertiary Piedmont Basin (NW Italy): the Alba section revisited. *Palaeogeography, Palaeoclimatology, Palaeoecology*, 310, 238–255.

Dietl, G.P., Kidwell, S.M., Brenner, M., Burney, D.A., Flessa, K.W., Jackson, S.T. & Koch, P.L. (2015) Conservation paleobiology: leveraging knowledge of the past to inform conservation and restoration. *Annual Review of Earth and Planetary Sciences*, 43, 79–103.

Eichenlaub, L.A. (2016) A fluid inclusion study of acidity in bedded halite of the Larne Halite Member, Triassic Mercia Mudstone Group from the Carnduff 2 Core, County Antrim, Northern Ireland. West Virginia University Graduate Theses, Dissertations, and Problem Reports no. 5532.

Eichenlaub, L.A., Benison, K.C. & Andeskie, A.S. (2016) Acid fluid inclusions in bedded halite of the Triassic Mercia Mudstone, Northern Ireland. Geological Society of America Annual Meeting, Abstracts with Programs.

Forster, A., Irmen, A.P. & Vondra, C. (1996) Structural interpretation of Sheep Mountain Anticline, Bighorn Basin, Wyoming. Wyoming Geological Association 47th Annual Field Conference Guidebook, 239–251.

Foster, T., Soreghan, G.S., Soreghan, M.J., Benison, K.C. & Elmore, R.D. (2014) Climatic and palaeogeographic significance of aeolian sediment in the Middle Permian Dog Creek Shale (Midcontinent U.S.). *Palaeogeography, Palaeoclimatology, Palaeoecology*, 402, 12–29.

Gastaldo, R.A., DiMichele, W.A. & Pfefferkorn, H.W. (1996) Out of the icehouse into the greenhouse: a Late Paleozoic analog for modern global vegetational change. *GSA Today*, 6(10), 1–7.

Gibson, M.E. & Benison, K.C. (2023) It's a Trap! The diversity and search for organic material in modern and ancient halite. *Journal of Sedimentary Research*, 93, 642–655.

Goldstein, R.H. (1998) Paleosols of Late Pennsylvanian cyclic strata, New Mexico. *Sedimentology*, 35(5), 777–803.

High, L.R. & Picard, M.D. (1969) Stratigraphic relations within upper Chugwater Group (Triassic), Wyoming. *The AAPG Bulletin*, 53, 1091–1104.

Hardie, L.A. & Eugster, H.P. (1971) The depositional environment of marine evaporites: a case for shallow, clastic accumulation. *Sedimentology*, 16(3), 187–220.

Holliday, D.W. (1970) The petrology of secondary gypsums: a review. *Journal of Sedimentary Petrology*, 40, 734–744.

Irmen, A.P. & Vondra, C.F. (2000) Aeolian sediments in lower to middle(?) Triassic rocks of central Wyoming. *Sedimentary Geology*, 132(1–2), 69–88.

Kipnis, E.L., Bowen, B.B., Hutchings, S.J., Hynek, S.A. & Benison, K.C. (2020) Major ion geochemistry in Na-Cl-Mg-K-Cl-SO_4 brines using portable X-ray fluorescence spectrometry. *Chemical Geology*, 558, 119865.

Kiro, Y., Goldstein, S.L., Lazar, B. & Stein, M. (2016) Environmental implications of salt facies in the Dead Sea. *GSA Bulletin*, 128, 824–841.

Knapp, J.P. (2020) *Alluvial fans, loess plains, lakes, and distributive fluvial systems: depositional systems of the Permian-Triassic red beds and evaporites of Wyoming (USA)*. Morgantown, West Virginia, USA: West Virginia University ProQuest Dissertations Publishing. 28353090.

Knapp, J.P., Benison, K.C. & Andeskie, A.S. (2016) Redbeds in Wyoming: reading late Permian-early Triassic environments and climates from the Red Peak and Crow Mountain Formations. Abstracts with Programs, Geological Society of America Annual Meeting.

Knapp, J.P., Benison, K.C. & Andeskie, A.S. (2015) Testing if thin carbonate units are marine or non-marine: applying the Hardie approach to the Triassic Alcova limestone of Wyoming. *GSA Abstracts with Programs*, 47(7), 504.

Langford, R.P., Gill, T.E. & Jones, S.B. (2016) Transport and mixing of eolian sand from local sources resulting in variations in grain size in a gypsum dune field, White Sands, New Mexico, USA. *Sedimentary Geology*, 333, 184–197.

Lovelace, D.M. & Lovelace, S.D. (2012) Paleoenvironments and paleoecology of a lower Triassic invertebrate and vertebrate ichnoassemblage from the Red Peak Formation (Chugwater Group), Central Wyoming. *Palaios*, 27(9), 636–657.

Lowenstein, T.K. & Hardie, L.A. (1985) Criteria for the recognition of saline pan evaporites. *Sedimentology*, 32(5), 627–644.

Lugli, S., Vinicio, M., Marco, R. & Schreiber, C.B. (2010) The primary lower gypsum in the Mediterranean: a new facies interpretation for the first stage of the Messinian salinity crisis. *Palaeogeography, Palaeoclimatology, Palaeoecology*, 297(1), 83–99.

Manzi, V., Lugli, S., Roveri, M. & Schreiber, B.C. (2009) A new facies model for the Upper Gypsum of Sicily (Italy): chronological and palaeoenvironmental constraints for the Messinian salinity crisis in the Mediterranean. *Sedimentology*, 56, 1937–1960.

Maughn, E.K. (1972) Geologic map of the Wedding of the Waters Quadrangle, Hot Springs County, Wyoming. US Geological Survey Map GQ-1042.

McKee, E.D. (1966) Structures of dunes at White Sands National Monument, New Mexico (and a comparison with structures of dunes from other selected areas). *Sedimentology*, 7(1), 3–69.

Middleton, G. (1973) Johannes Walther's law of the correlation of facies. *GSA Bulletin*, 84, 979–988.

Montañez, I.P. & Poulsen, J.P. (2013) The Late Paleozoic ice age: an evolving paradigm. *Annual Review of Earth and Planetary Sciences*, 41, 629–656.

Mormile, M.R., Hong, B.Y. & Benison, K.C. (2009) Molecular analysis of the microbial communites of Mars-analog lakes in Western Australia. *Astrobiology*, 9, 919–930.

Noffke, N., Gerdes, G., Klenke, T. & Krumbein, W.E. (2001) Microbially induced sedimentary structures: a new category within the classification of primary sedimentary structures. *Journal of Sedimentary Research*, 71(5), 649–656.

Parrish, J.T. (1995) Geologic evidence of permian climate. In: Scholle, P.A., Peryt, T.M. & Ulmer-Scholle, D.S. (Eds.) *The Permian of Northern Pangea*. Berlin, Germany: Springer-Verlag, pp. 53–62.

Payne, J.L. & Clapham, M.E. (2012) End-Permian mass extinction in the oceans: an ancient analog for the twenty-first century? *Annual Review of Earth and Planetary Sciences*, 40, 89–111.

Petras, B. (2021) *Refining the sedimentology and geochemistry of the Mid-Permian Blaine Formation of the Rebecca K. Bounds Core from Greeley County, Kansas, West Virginia*. Morgantown, West Virginia, USA: University ProQuest Dissertations Publishing, 28653037.

Picard, M.D. (1967) Stratigraphy and depositional environments of the Red Peak member of the Chugwater Formation (Triassic), west-central Wyoming. *Rocky Mountain Geology*, 6(1), 39–67.

Sanchez Botero, C.A., Oboh-Ikuenoby, F.E., Grabel, L. & Adojoh, O.C. (2021) Palynomorphs in southern Western Australia lake sediments: evidence of climate change and hypersalinity during the Cenozoic. *Palynology*, 45(2), 201–214.

Schreiber, B.C. (1987) Environments of subaqueous gypsum deposition. *SEPM Marine Evaporites*, SC4, 43–72.

Schreiber, B.C. & El Tabakh, M.E. (2000) Deposition and early alteration of evaporites. *Sedimentology*, 47, 215–238.

Schreiber, B.C. & Kinsman, D.J. (1975) New observations on the Pleistocene evaporites of Montallegro, Sicily and a modern analog. *Journal of Sedimentary Petrology*, 45(2), 469–479.

Schreiber, B.C., Friedman, G.M., Decima, A. & Schreiber, E. (1976) Depositional environments of Upper Miocene (Messinian) evaporite deposits of the Sicilian Basin. *Sedimentology*, 23, 729–760.

Smoot, J.P. & Castens-Seidell, B. (1994) Sedimentary features produced by efflorescent salt crusts, Saline Valley and Death Valley, California. In: *Sedimentology and geochemistry of modern and ancient saline lakes*. Claremore, Oklahoma, USA: SEPM Society for Sedimentary Geology, 50, 73–90.

Smoot, J.P. & Lowenstein, T.K. (1991) Depositional environments of non-marine evaporites. In: Melvin, J.L. (Ed.) *Evaporites Petroleum and Minerals Resources, Developments in Sedimentology*. New York, New York, USA: Elsevier, 50, 189–347.

Stanley, S.M. & Yang, X. (1994) A double mass extinction at the end of the Paleozoic Era. *Science*, 266, 1340–1344.

Sweet, A.C., Soreghan, G.S., Sweet, D.E., Soreghan, M.J. & Madden, A.J. (2013) Permian dust in Oklahoma: source and origin for Middle Permian (Flowerpot-Blaine) redbeds in Western Tropical Pangaea. *Sedimentary Geology*, 284–285, 181–195.

Tomlinson, C.W. (1916) The origin of red beds: a study of the conditions of origin of the Permo-Carboniferous and Triassic red beds of the western United States. *The Journal of Geology*, 24(3), 238–253.

Vajda, V., McLoughlin, S., Mays, C., Frank, T.D., Fielding, C.R., Tevyaw, A., Lehsten, V., Bocking, M. & Nicoll, R.S. (2020) End-Permian (252 Mya) deforestation, wildfires, and flooding—An ancient biotic crisis with lessons for the present. *Earth and Planetary Science Letters*, 529, 1–12.

Zaikova, E., Benison, K.C., Mormile, M.R. & Johnson, S.S. (2018) Microbial communities and their predicted metabolic functions in a desiccating acid salt lake. *Extremophiles*, 22, 367–379.

Zambito, J.J. & Benison, K.C. (2013) Extremely high temperatures and paleoclimate trends recorded in Permian ephemeral lake halite. *Geology*, 41(5), 587–590.

Zambito, J.J., Benison, K.C., Foster, T.M., Soreghan, G.S., Soreghan, M.J. & Kane, M. (2012) Lithostratigraphy of Permian red beds and evaporites in the Rebecca K. Bounds Core, Greeley County, Kansas. Kansas Geological Survey Open File Report 2012-15.

How to cite this article: Bradford, M.Y. & Benison, K.C. (2024) Gypsum lakes, sandflats and soils revealed from the Triassic Red Peak Formation of the Chugwater Group, north-central Wyoming. *The Depositional Record*, 00, 1–19. Available from: https://doi.org/10.1002/dep2.273